



ANCHORAGE OF STRUCTURAL OR NON STRUCTURAL COMPONENTS FOR USUAL BUILDINGS IN SEISMIC AREA

Eric FOURNELY¹ and Philippe BRESSOLETTE²

ABSTRACT

On site joints of prefabricated elements are often realized with mechanical anchors; it is specifically the case for wooden houses. The anchors are particularly important for buildings undergoing seismic loads. On one hand, this study presents experimental results obtained on tests carried out on different types of concrete specimens with mechanical expansion anchors. Different loading histories are also applied in this experimental approach. Load-displacement curve, residual strength and failure modes are observed. On the other hand, two numerical models are developed in order to reach non linear load-displacement curves of anchorage and damage of concrete. Hypothesis and results of these different approaches are presented and a comparison between models and between experimental and numerical results are performed.

INTRODUCTION

Constructive solutions using prefabricated elements often use mechanical anchors post-installed on site. For seismic design situations, under the umbrella of capacity design with development of targeted cyclic plastic zones and other zones oversizing, anchors shall stay in elastic domain. It is for example the case for timber frames with mechanical anchors in wall ties or wooden bracings with anchors in basement (Fournely et al., 2011). Figure 1 gives an illustration of these kinds of anchorage.

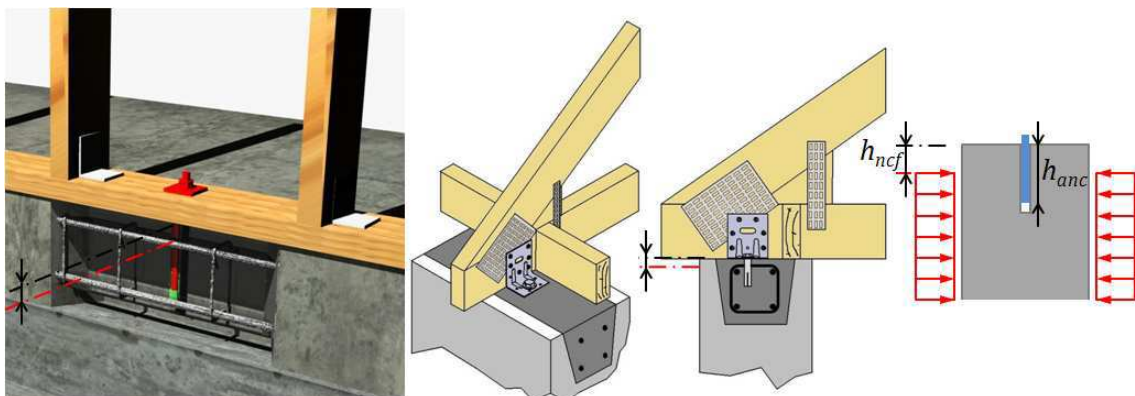


Figure 1. Example of two types of mechanical anchorage for wooden components of usual building in reinforced concrete ties.

¹ Dr, Clermont Université, Université Blaise Pascal, Institut Pascal, BP 10448, F-63000 Clermont-Ferrand & CNRS, UMR 6602, Institut Pascal, F-63171 Aubière, France, e.fournely@polytech.univ-bpclermont.fr

² Dr-Ing, Clermont Université, Université Blaise Pascal, Institut Pascal, BP 10448, F-63000 Clermont-Ferrand & CNRS, UMR 6602, Institut Pascal, F-63171 Aubière, France, ph.bressollette@polytech.univ-bpclermont.fr

The proposed study is based on experimental results and on finite element simulations. Experimental approach is carried out on two sizes of cylindrical specimens, 16 and 25 cm diameter. Two axial externally threaded anchors are set up on each specimen and they are loaded in monotonic or cyclic tension. The strength and, more generally, the mechanical behavior of each anchorage is recorded and studied. The finite element simulation is performed with two different modellings: one in “2D” axisymmetric mode for pure traction and one in 3D in view of introducing imperfections on the location of the anchorage component (Torre-Casanova et al., 2012).

The configurations, the hypothesis and the results of these experimental and numerical approaches are presented and analyzed in this study. The effect of confinement is particularly studied and discussed in order to appreciate to reliability of this kind of assemblies.

2 EXPERIMENTAL STUDY

The experimental campaign is carried out on cylindrical concrete specimens, outfitted with externally threaded anchors (Hilti HST M8x75/10). The dimensions of the two kinds of concrete specimens are 16 cm in diameter with 32 cm in high, and a diameter of 30 cm with a high of 40 cm. The anchors are located along the longitudinal axle of the specimen on each face. Dimension of the hole (diameter, length) are those given in technical manual of Hilti firm (Hilti, 2013). The specimens are not reinforced and the effect of confinement varies with the diameter of the specimen. The set up of this experimentation is illustrated on figure 2. Figure 3 gives information on the anchorage itself and on the installation process.

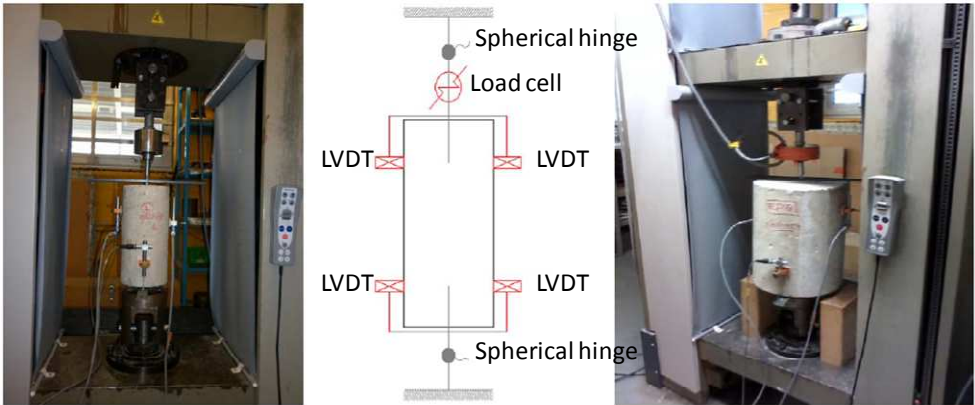


Figure 2. Experimental setup

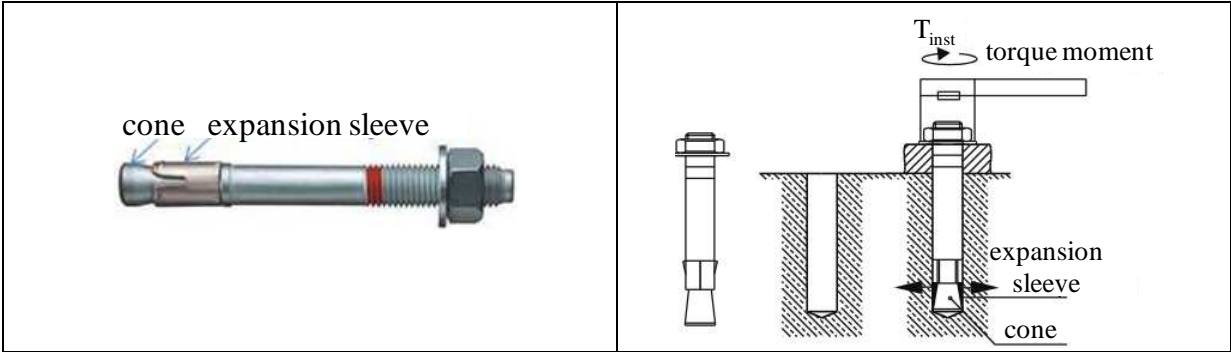


Figure 3. Anchor configuration

Mechanical and geometrical parameters are given in table 1 in order to define the concrete characteristics and dimension and the location of the hole for the anchorage. The low value of standard deviation of the parameters can be noted. Values of f_c for concrete are determined on matched

specimens realized at the same time as the specimens tested with anchors. 12 16x32 specimens and 12 30x40 specimens are realized for anchors tests and 10 specimens are tested in compression (Livolsi, 2011).

Table 1. Geometrical and mechanical characteristics of concrete specimens

	concrete			anchor		
	slump test (cm)	strength		hole depth (mm)	drilling angle (deg)	centering drill (mm)
		compression (MPa)	tension (MPa)			
mean value	6.4	28.9	2.8	71	0.4	2
standard deviation	0.7	1.1	0.5	3	0.1	2

The applied loads are monotonic, with different rates, or cyclic fitted to the normative requirements. Tests are carried out with global imposed displacements. The specific behavior of each anchor is recorded, but the load history (in displacement) integrates the effect of the behavior of the two anchors put in a specimen. The effect of the mass of the specimen is integrated in the value of the load applied on the upper and the lower anchor of a specimen. For each specimen dimension set, 4 tests are carried out with a low rate monotonic displacement (x mm/mn), 4 with a rapid monotonic loading (y mm/mn) and 4 with increasing cyclic sequences signal as shown on figure 4.

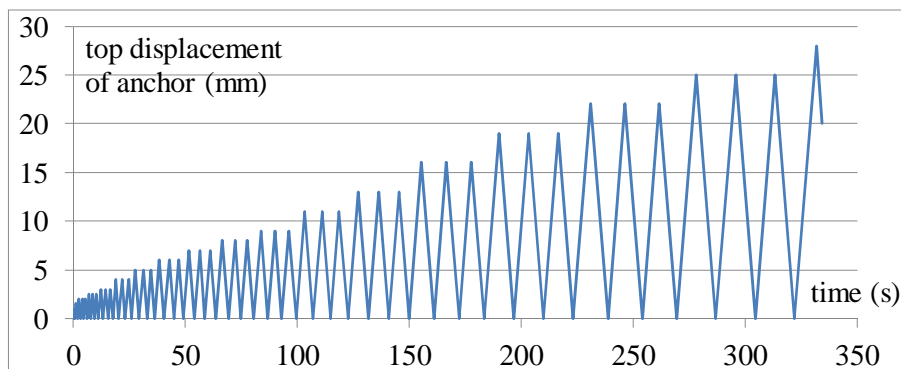


Figure 4. Specific cyclic loading history

The behavior is locally and globally analyzed: appearance of cracks, slip measurement between concrete and anchor, strength, damage... Elements of mechanical behavior are given on table 2 and on figures 5 and 6. Figure 5 gives examples of curves obtained for 16x32 and 30x40 specimens with monotonic and increasing cyclic loadings. The collapse is well distributed between the upper and the lower anchor as indicated in table 2. The modes of failure (cracks in concrete or extraction-slip of anchors) are also well distributed for 16x32 specimens, but for 30x40 specimens, the strength is mainly dependant of pull-out friction. Regarding the different loadings and sizes of specimens, the strength increases with the diameter of specimen and decreases with the rate of loading while the standard deviation varies between 10% for monotonic loadings to 30% for cyclic ones.

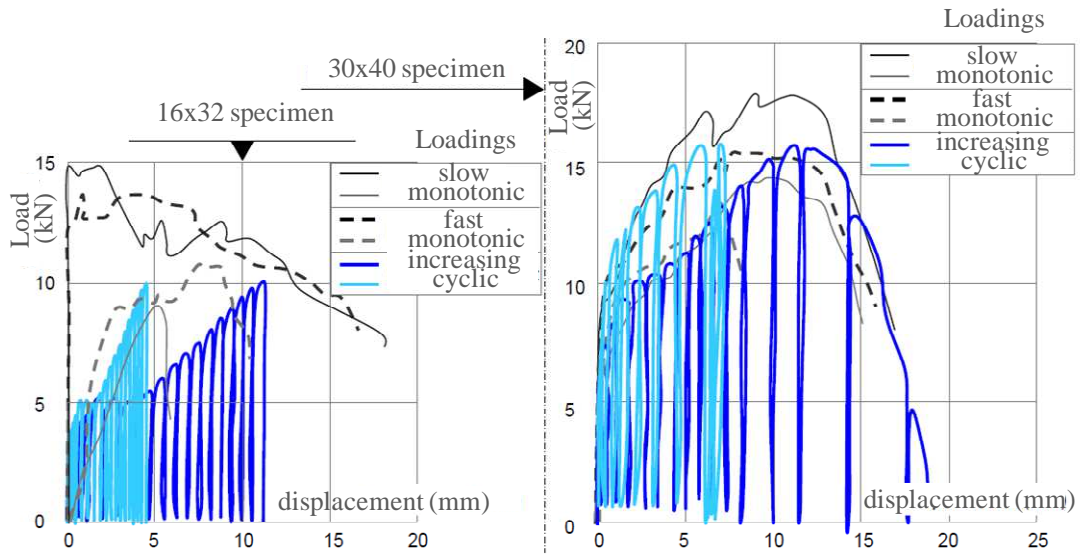


Figure 5. Example of experimental results for monotonic and increasing cyclic loadings

Table 2. Experimental results

		16x32			30x40		
		maximum of load Fmax (kN)			maximum of load Fmax (kN)		
		mean value	standard deviation	gap with slow rate results	mean value & gap / (16x32)	standard deviation	gap with slow rate results
monotonic loading	slow rate	12.9	1.2		16.7 (+29%)	1.2	
	rapid rate	12.4	1	-4%	15.1 (+22%)	0.1	-9%
specific cyclic loading		11.1	3.2	-14%	12.2 (+10%)	1.3	-27%
		displacement for Fmax (mm)			displacement for Fmax (mm)		
		mean value	standard deviation	gap with slow rate results	mean value & gap / (16x32)	standard deviation	gap with slow rate results
monotonic loading	slow rate	6.9	1.9		6.1 (-11%)	1.3	
	rapid rate	6.1	2.3	-11%	7.5 (+23%)	3.2	+24%
specific cyclic loading		10	5.4	+45%	12.5 (+25%)	7.5	+106%



Figure 6. Illustration of failure modes

NUMERICAL MODELLING

FEM modeling is divided in two approaches, one in “2D” axisymmetric mode for pure traction and one in 3D in view of introducing imperfections on the location of the anchorage component, cf. figure 7. 4 120 elements are included in the axisymmetric model and 25 960 elements are needed for the 3D mesh. Numerical modeling takes into account the friction between concrete and anchor (Coulomb friction) and damage of concrete with regularized Mazars’s model (Mazars, 1984) (La Borderie, 2003), with different configurations of concrete confinement. Elementary parameters are defined from results of compression tests (f_{cj} ...) or taken in literature (friction ratio...). Calculations are conducted with CAST3M software in two phases corresponding to a preloading and then a mechanical loading.

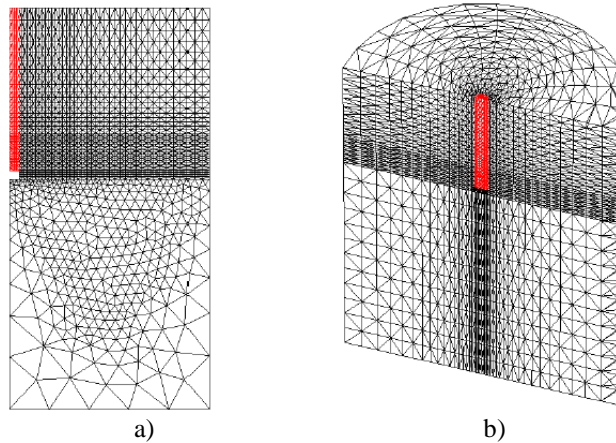


Figure 7. FE modeling: a) axisymmetric mesh, b) 3D mesh,

Preloading

The tightening torque of the anchorage is modeled by a initial thermal loading. For the 3D model, figure 8 illustrates this thermal loading equivalent to torque sequence. Temperature varies linearly in order to simulate the shape variation of the expansive sleeve of the anchor. The maximum value of temperature is calibrated to correspond of the anchor setup prescription.

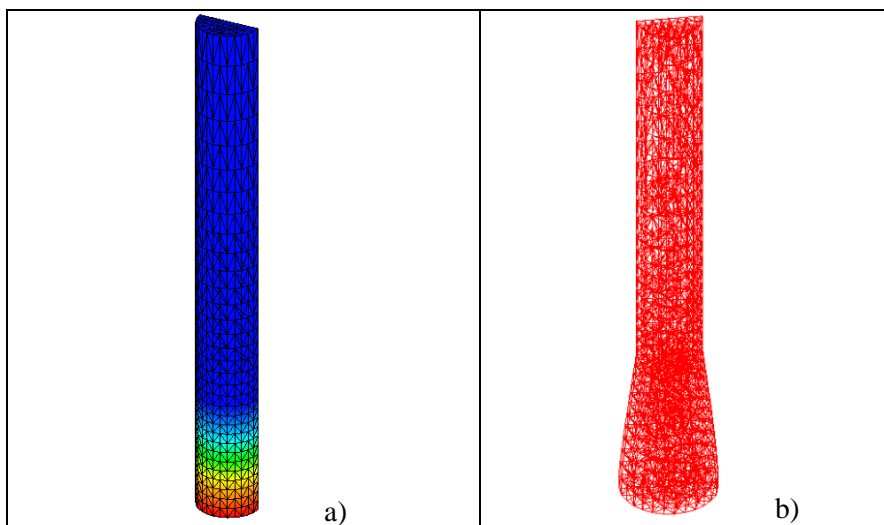


Figure 8 mesh of the anchor, a) temperature map, b) dilatation

Mechanical loading

This second loading corresponds to imposed axial displacement of the upper part of the anchor with a step by step procedure. Due to the different non linearities, the convergence of the non linear MEF computation is difficult; the erratic nature of the force-displacement curve (Figure 9) exhibits these convergence difficulties.

Numerical results

The curves presented on figure 9 exhibit a first part of behavior quasi elastic with a light softening and then a second part corresponding to successive slip between anchor and concrete. A similar behavior is obtained for the two diameter values of tested specimens, even if the gap observed on experimental strength for these two configurations is slightly greater than the one given by numerical models.

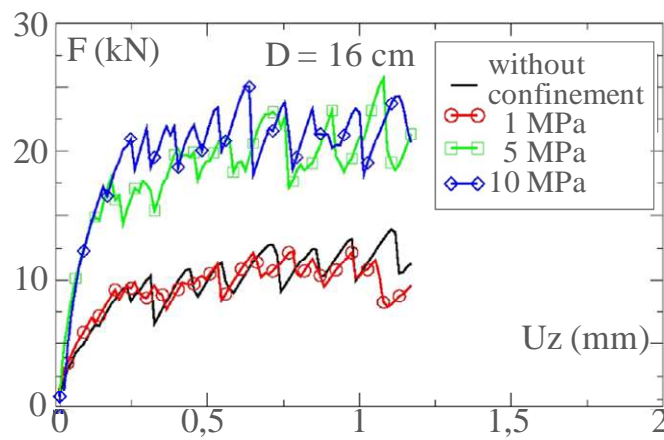


Figure 9. Mechanical behavior of anchorage in 16 diameter specimens with different confinement pressures

Nevertheless, the experimental and numerical breakout force-displacement curves are similar both in their pattern-ship than in singular values. Taking into account a lateral confining pressure allows to highlight its influence on the global behavior of the anchorage. Numerical results exhibit also a threshold effect on lateral pressure on the pullout strength, which can be multiplied by two (fig. 9). Indeed, we can observe that 1MPa lateral pressure does not significantly affect the load-displacement curve. In a same way, there is no important difference between 5 and 10 MPa confinement effects.

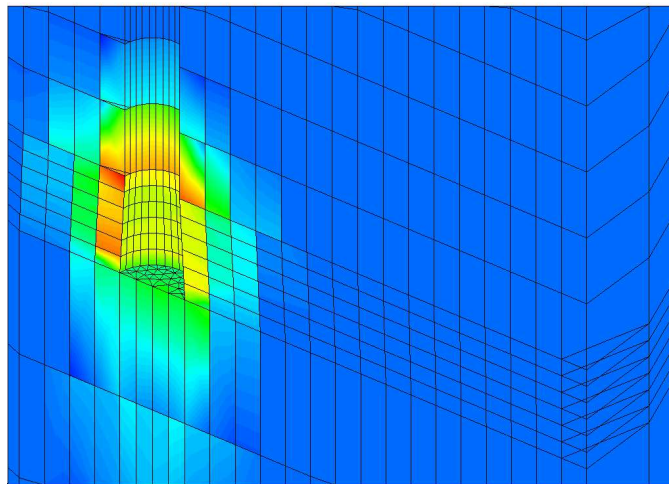


Figure 10. Example of damage map for with 3D model

Figures 10 and 11 give illustrations of damage results with 3D and 2D models. Figure 10 is given as an example of "3D map" obtained. The analysis of these 3D maps implies 2D projections or scalar evaluations like index damaged volume for a specific loading level. The damaged volume obtained with 3D and 2D models are quite comparable. For a 0.6 value of damage threshold, the difference of damaged volume is less than 20 % at the end of loading.

For the further comments, 2D model is used. Figure 11 presents for a same imposed displacement 4 maps of damage: without confinement and for 1, 5 and 10 MPa values of lateral pressure. On these maps, the conclusions on the effect of confinement drawn from figure 9 are confirmed.

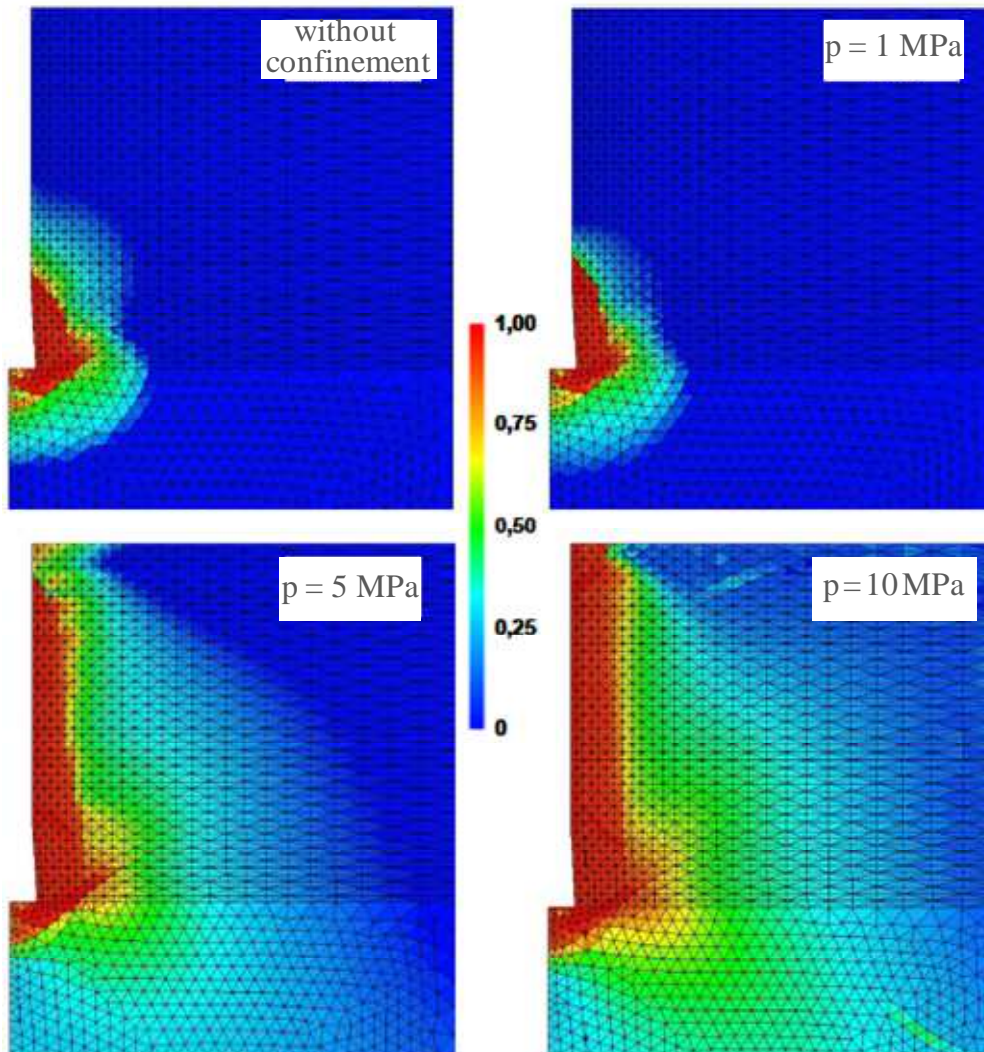


Figure 11. Damage maps in different configurations of confinement for 16cm diameter specimen

CONCLUSION

This study presents tests carried out on two sizes of specimens. Results in terms of relationship between load and displacement are obtained and failure modes are pointed out. The hypothesis of FEM models developed in this study are presented. Results of modeling are in a good accordance with experimental results and results of 2D and 3D models fit well for an axial loading. The analysis of damage map or damaged volume is an interesting element to study the residual strength and the

reliability of these kinds of assemblies. In the case of a combination of axial and tangential loading, only 3D model can be used. At the moment, the models are applied for monotonic loading. Further studies will be performed on one hand on experimental approaches and on the other hand on numerical developments. Specimens with reinforced concrete will be tested in order to identify the relation between lateral pressure and ties and stirrups. The numerical models will be tested with combined loadings (3D model) and also with cyclic loadings (2D and 3D models), closer to seismic situations. Finally, a stochastic approach to compute the statistical moments of the output parameters and build surface responses in order to determine the probability density functions and to carry out a sensitivity analysis will be developed.

REFERENCES

- Fournely E., Bressolette Ph., Livolsi G. (2011) « *Ancrage de composants de structures sur support en béton armé pour des ouvrages courants en zone sismique* », Colloque « Vers une maîtrise durable du risque sismique » AFPS'11, Marne-la-Vallée, 12-13 septembre 2011, pp. 59-68.
- Hilti INC (2013) Hilti Kwik bolt TZ carbon and stainless steel anchors in cracked and uncracked concrete *ICC-ES Evaluation Report ESR-1917*: 1-17
- La Borderie, Ch. (2003). Stratégies et modèles de calculs pour les structures en béton. Habilitation à diriger les Recherches, Université de Pau, France.
- Livolsi G. (2011) Ancrage dans un chaînage, paramètres influant sur son comportement mécanique, *Mémoire d'ingénieur Génie Civil, Polytech' Clermont Ferrand*
- Mazars, J. (1984). Application de la mécanique de l'endommagement au comportement non-linéaire et à la rupture de béton de structure. Thèse de Doctorat de l'Université Pierre et Marie Curie, Paris.
- Torre-Casanova A, Jason L, Davenne L, Pinelli X (2012). Confinement effects on the steel-concrete bond strength and pull-out failure, *Engineering fracture mechanics*, pp. 92-105.